

Analyst

Accepted Manuscript



This is an *Accepted Manuscript*, which has been through the Royal Society of Chemistry peer review process and has been accepted for publication.

Accepted Manuscripts are published online shortly after acceptance, before technical editing, formatting and proof reading. Using this free service, authors can make their results available to the community, in citable form, before we publish the edited article. We will replace this *Accepted Manuscript* with the edited and formatted *Advance Article* as soon as it is available.

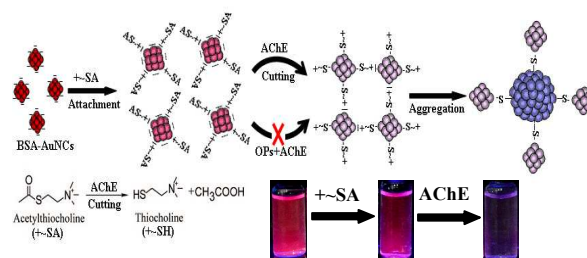
You can find more information about *Accepted Manuscripts* in the [Information for Authors](#).

Please note that technical editing may introduce minor changes to the text and/or graphics, which may alter content. The journal's standard [Terms & Conditions](#) and the [Ethical guidelines](#) still apply. In no event shall the Royal Society of Chemistry be held responsible for any errors or omissions in this *Accepted Manuscript* or any consequences arising from the use of any information it contains.

The Table of Contents:

Lab-on-a-Drop: Biocompatible Fluorescent Nanoprobes of Gold Nanoclusters for Label-Free Evaluation of Phosphorylation-Induced Inhibition of Acetylcholinesterase Activities Towards the Ultrasensitive Detection of Pesticide Residues

Ning Zhang,^a Yanmei Si,^a Zongzhao Sun,^a Shuai Li,^a Shuying Li,^a Yuehe Lin^b, and Hua Wang^{*a}



The hydrolytic catalysis and phosphorylation-induced inhibition of acetylcholinesterase were monitored using fluorescent BSA-AuNCs nanoprobes towards “lab-on-a-drop”-based detection of pesticide residues.

Cite this: DOI: 10.1039/c0xx00000x

www.rsc.org/xxxxxx

ARTICLE TYPE

Lab-on-a-Drop: Biocompatible Fluorescent Nanoprobes of Gold Nanoclusters for Label-Free Evaluation of Phosphorylation-Induced Inhibition of Acetylcholinesterase Activities Towards the Ultrasensitive Detection of Pesticide Residues

Ning Zhang,^a Yanmei Si,^a Zongzhao Sun,^a Shuai Li,^a Shuying Li,^a Yuehe Lin^b and Hua Wang^{*a}

Received (in XXX, XXX) Xth XXXXXXXXX 20XX, Accepted Xth XXXXXXXXX 20XX

DOI: 10.1039/b000000x

A simple, sensitive, selective, and “lab-on-a-drop”-based fluorimetric protocol has been proposed using biocompatible fluorescent nanoprobes of gold nanoclusters (AuNCs) for the label-free evaluation of the catalysis activity and phosphorylation of acetylcholinesterase (AChE) under physiologically-simulated environments. Protein-stabilized AuNCs were prepared to be mixed with acetylthiocholine (ATC) serving as “a drop” of fluorimetric reaction substrate. The AChE-catalyzed hydrolysis of ATC could release thiocholine to cause the aggregation of AuNCs towards a dramatic decrease in fluorescence intensities, which could be curbed by the phosphorylation-induced inhibition of AChE activities when exposed to organophosphorus compounds (OPs). The reaction procedures and conditions of AChE catalysis and phosphorylation were monitored by fluorimetric measurements and electron microscopy imaging. Moreover, a selective and ultrasensitive fluorimetric assay has been tailored for the detection of pesticide residues using dimethyl-dichloro-vinyl phosphate (DDVP) as an example. Investigation results indicate that the specific catalysis and irreversible OP-induced phosphorylation of AChE, in combination with sensitive fluorimetric outputs, could facilitate the detection of total free OPs with high selectivity and sensitivity. A linear concentrations of DDVP ranging from 0.032 nM to 20 nM could be obtained with a detection limit of 13.67 pM. Particularly, pesticide residues of DDVP in vegetable samples were quantified down to ~ 36 pM. Such a label-free “lab-on-a drop”-based fluorimetry may promise wide applications for the evaluation of physiologic catalysis activities of various enzymes (i.e., cholinesterase), and especially for monitoring the direct phosphorylation biomarkers of free OPs towards rapid and early warning and accurate diagnosis of OP exposures.

1. Introduction

Highly toxic organophosphorus compounds (OPs), including nerve agents and organophosphate pesticides, are severely threatening public safety and environment. Nerve agents as toxic chemical warfare agents¹ are commonly misused in modern war and terrorist attack, such as Tokyo subway attack in 1995 and Syria events in 2013. In particular, pesticides are used worldwide in the agriculture leading to the widespread contamination in air, water, soil and agricultural products.² As a way of invading and attacking human body, OPs may bind to cholinesterase like acetylcholinesterase (AChE) at certain active sites of amine acids (i.e., serine) inducing the inhibition of the catalysis activities of AChE.¹ And the phosphorylation-induced inactivation of AChE in body can bring to the accumulation of neurotransmitter acetylcholine in vivo, resulting in the disturbance of cholinergic receptor activity to serious clinical complications (i.e., respiratory tract and fibrillation) and even to death.³ Therefore, the

development of rapid, sensitive, and selective detection methods is urgently desirable for the evaluation of catalysis and phosphorylation of AChE especially monitoring of OPs towards the rapid early warning and accurate diagnosis of OP exposures.

Up to date, numerous detection strategies have been widely applied for monitoring OP exposures,⁴⁻²⁰ especially the ones for quantifying the direct biomarkers of OP exposures of free OPs based on the specific OP-induced inhibition of catalysis activities of AChE that are recognized to be highly sensitive and selective.^{9, 11, 13, 15, 16, 20} These measurement methods for OP tests mainly include gas chromatography (GC),⁴⁻⁶ high performance liquid chromatography (HPLC),^{7, 8} electrochemical tests,⁹⁻¹¹ colorimetric assays,¹²⁻¹⁴ and fluorescent detections.¹⁵⁻²⁰ Comparing to the chromatography evaluations and electrochemical analysis methods that need either time-consuming operation or complicated labelling and modification procedures, the fluorimetric methodologies stand out as the rapid, sensitive, and efficient ones especially in combination with the nanotechnologies and fluorescent nanomaterials, most known as

Analyst Accepted Manuscript

semiconductor quantum dots (QDs).^{15, 18, 20} Inorganic fluorescent nanomaterials can possess some advantages over the traditional organic fluorescent dyes, including high fluorescence intensity, good stability, spectral line width, and sustainable luminous, making them increasingly used as fluorescent nanoprobe for detecting various OP biomarkers in biomedicine, food hygiene, and environmental monitoring.¹⁸⁻²⁰ Typically, some fluorescence assays have employed QDs for detection of free OPs including the evaluation of AChE activities.^{15, 18, 20} For example, Yu et al have proposed a sensitive sensing system for the analysis of OPs with photoluminescent QDs.¹⁸ Zheng and coworkers described the pesticide biosensors using nanostructured AChE films and CdTe QDs.²⁰ The use of QDs of heavy metal ion, however, may suffer from the potential toxicity and complicated synthesis procedures.¹⁹ In particular, the labelling or release of heavy metals ion during the procedures of enzyme-catalysis reactions may cause the denaturation and the activity inhibition of cholinesterase (i.e., AChE), in addition to potential environmental endangerments.¹⁹⁻²¹ Accordingly, developing more reliable, label-free, and continuous investigation systems alternatively using biocompatible fluorescent probes to achieve physiologically friendly “green” reaction environments to achieve the better evaluation of the catalysis and phosphorylation of AChE and the AChE-based analysis of OPs is of great interest.

Recent years, there have emerged new kinds of fluorescent nanomaterials of noble metal nanoclusters, such as gold nanoclusters (AuNCs) and silver nanoclusters.²²⁻²⁸ These nanoclusters possess some unique properties of ultra-small size, non-toxicity, high biocompatibility, and strong fluorescence. However, most of the intensive applications are found for the analysis of routine substances such as heavy metal ions, dopamine, and glucose.^{22-25, 27, 28} For example, Zhang et al reported a selective method for the detection of Cu²⁺ using glutathione-protected fluorescent AuNCs.²² Alternatively, in this work, a sensitive, simple, and rapid fluorimetric method has been proposed by way of “lab-on-a-drop” with biocompatible AuNCs as highly fluorescent nanoprobe for the label-free evaluation of the catalysis and OP-induced inhibition of AChE activities towards the quantitative determination of OPs. The main fluorimetric analysis procedure is illustrated schematically in **Scheme 1**. Herein, bovine serum albumin (BSA)-stabilized gold nanoclusters (BSA-AuNCs) were prepared to be mixed with acetylthiocholine (ATC) to serve as “a drop” of fluorimetric reaction substrate for probing the catalysis activities and phosphorylation of AChE and further detecting of OPs using dimethyl-dichloro-vinyl phosphate (DDVP) as an OP model. The release of thiocholine from the AChE-catalyzed hydrolysis of ATC would cause the aggregation of AuNCs so as to decrease their fluorescence intensities, depending on the catalysis activities of AChE. Moreover, the presence of OPs (i.e., DDVP) in the reaction system could conduct the specific inhibition of AChE activities, so that highly sensitive and selective quantification of OPs could be expected. To the best of our knowledge, this is the first report the label-free systematic evaluation of catalysis activities and phosphorylation reactions of AChE has been realized under physiologically friendly environments by way of “lab-on-a-drop” with biocompatible fluorescent nanoprobe of AuNCs in combination with sensitive fluorimetric outputs. The

application feasibility of the AuNCs-based fluorimetry for quantifying low-level OP residues in vegetable samples has been demonstrated with high detection sensitivity and selectivity.

2. Experimental section

2.1. Chemicals and materials

Tetrachloroauric (III) acid (HAuCl₄·3H₂O, > 99.9%), bovine serum albumin (BSA), acetylthiocholine (ATC), acetylcholinesterase (AChE) were purchased from Sigma-Aldrich (Beijing, China). Dimethyl-dichloro-vinyl phosphate (DDVP) was provided by Dibai Reagents (Shanghai, China). vitamin C (V_C), vitamin B1 (V_{B1}), vitamin B2 (V_{B2}), FeCl₃, NaCl, MgCl₂, ZnCl₂, KCl, CaCl₂, Na₃PO₄, glucose (Glu), and fructose (Fru) were purchased from Beijing Chemical Reagent Co. (Beijing, China). All chemicals used were of analytical grade, and all glass containers were cleaned by aqua regia and ultrapure water.

2.2. Apparatus

The fluorescence measurements were conducted using fluorescence spectrophotometer (F-7000, Hitachi, Japan) operated at an excitation wavelength at 470 nm, with both excitation and emission slit widths of 5.0 nm. The fluorescence intensities were collected at ~ 634 nm. Transmission electron microscopy (TEM, Tecnai G20, FEI, USA) images were recorded by operating at 100 kV. High-performance liquid chromatography (HPLC) (Agilent 1200, USA) analysis was performed on a Zorbax SB-C18 column (150 mm × 4.6 mm).

2.3. Synthesis of protein-stabilized Au nanoclusters

The protein-stabilized fluorescent Au nanoclusters (AuNCs) were prepared with BSA as the protein stabilization and reduction agents following a modified synthetic route reported previously.²⁶ Briefly, aqueous HAuCl₄ solution (1.0 mL, 10 mM) was added to BSA solution (1.0 mL, 50 mg/mL) under vigorous stirring at 37 °C for 10 min. Then, NaOH solution (0.10 mL, 1.0 M) was introduced to be further vigorously stirred at 37 °C for 12 h. Finally, the resulting solution was dialyzed in water for 48 h. The BSA-stabilized AuNCs was stored at 4 °C for future usage.

2.4. Preparation of stock OP solutions of DDVP

The stock solution of OPs was prepared by using DDVP as an example. An aliquot of DDVP was dissolved in 5.0 mL hexane and stored in refrigerator at 4 °C for further use. Different DDVP concentrations were obtained by freshly diluting DDVP stock solution with isopropanol.

2.5. Fluorimetric evaluations of AChE catalysis activities

An aliquot of fluorimetric reaction substrate consisting of 225 μL AuNCs (1.25 mM) and 25 μL ATC (500 μM) was added into six tubes (0.5 mL). Each of 25 μL AChE solutions with different catalysis activities of 0.0, 0.00005, 0.0005, 0.0050, 0.050, 0.50 U / mL was then introduced. Following that, the resulting mixtures

of catalysis reactions were separately incubated at 37 °C for 1 h. Subsequently, the fluorescence spectra of the reaction mixtures were recorded depending on the catalysis activities of AChE. Herein, the quenching efficiencies of AuNCs by thiocholine released from the AChE-catalyzed ATC hydrolysis were calculated according to the equation: Quenching efficiency = $(F_0 - F) / F_0$, in which F_0 and F refer to the fluorescence intensities of AuNC nanoprobe reached the maximum before and after AChE-catalytic ATC reactions at different conditions, respectively.

2.6. Fluorimetric analysis of DDVP

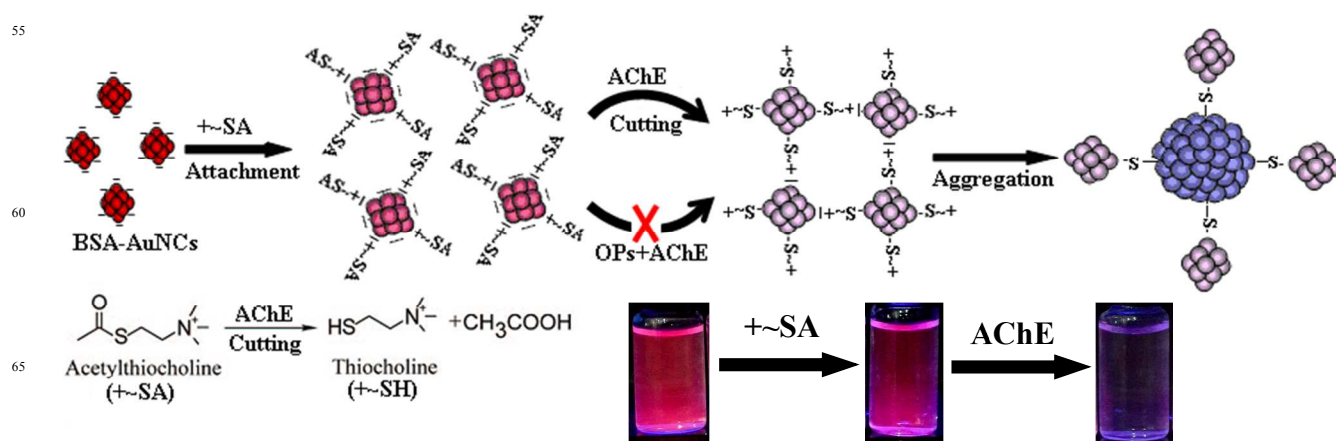
An aliquot of 25 μL DDVP solutions with different concentrations (0.0 , 3.2×10^{-5} , 1.6×10^{-4} , 0.8×10^{-3} , 0.4×10^{-2} , and $2.0 \times 10^{-2} \mu\text{M}$) was mixed with 25 μL AChE ($0.5 \text{ U} / \text{mL}$) to be incubated for 1 h. An amount of fluorimetric reaction substrate consisting of 225 μL AuNCs (1.25 mM) and 25 μL ATC ($500 \mu\text{M}$) was introduced to each of the above reactant solutions to be incubated at 37 °C for 1 h. Furthermore, the fluorescence spectra of the reaction mixtures were recorded at $\sim 634 \text{ nm}$. The DDVP inhibition efficiencies of AChE catalysis were calculated according to the equation: Inhibition efficiency = $(F_x - F) / (F_0 - F)$,¹⁶ in which F_0 refers to the fluorescence intensities of “a drop” of fluorimetric reaction substrate consisting of AuNCs with ATC; and F and F_x refer to the fluorescence intensities of AuNC nanoprobe with AChE-catalytic ATC reaction substrates in the absence and presence of DDVP, respectively.

Moreover, the detection selectivity of the developed fluorimetric assay for DDVP was examined accordingly for

potential interferents of $0.020 \mu\text{M}$ vitamin C (Vc), vitamin B1 (V_{B1}), vitamin B₂ (V_{B2}), Fe^{3+} , Na^+ , Mg^{2+} , Zn^{2+} , K^+ , Ca^{2+} , PO_4^{3-} , glucose (Glu), and fructose (Fru), comparing to $0.0040 \mu\text{M}$ DDVP.

2.7. Preparation and analysis of vegetable samples of DDVP residues

Vegetable samples of Chinese cabbage were pre-treated on site in vegetable field with DDVP, and then experimentally processed according to a modified procedure.²⁹ Briefly, 20 g of DDVP-treated samples of Chinese cabbage were finely chopped, and then dissolved in 100 mL methanol to be ultra-sonicated for 60 min. After that, the sample mixtures were centrifuged to get the supernatants and further filtered, of which the impurities such as pigments in the filtrates were removed with activated carbon. Following that, the DDVP residues-containing samples were washed with 20 mL methanol, and then dried at 50 °C by vacuum rotary evaporator. The concentrations of DDVP residues in samples were measured by using high-performance liquid chromatography (HPLC) (Agilent 1200, USA), with Zorbax SB-C18 columns at 25 °C. Moreover, a certain amount of DDVP sample with the measured concentration was diluted into different concentrations of DDVP residues for the fluorimetric assays, according to the same analysis procedure above. In addition, the detections of some DDVP-containing vegetable samples were comparably conducted by the HPLC and the fluorimetric assay.



Scheme 1 Schematic illustration of the fluorimetric assay procedure with fluorescent changes of BSA-stabilized AuNCs (BSA-AuNCs), including the AChE-catalyzed hydrolysis of ATC and the phosphorylation-induced inhibition of AChE catalysis activities by OPs.

3. Results and discussion

3.1. The detection mechanism and procedure of the “lab-on-a-drop”-based fluorimetric method

The fluorimetric assay procedure using fluorescent nanoprobe of AuNCs is illustrated schematically in **Scheme 1**, including the AChE-catalyzed hydrolysis of ATC and the OP-induced inhibition of AChE catalysis activities. Here, BSA-stabilized AuNCs (BSA-AuNCs) that were synthesized at about pH 12 were

negatively charged, since the isoelectric point of BSA capped on AuNCs is pH 4.7.³⁰ Once positively-charged ATC was introduced, it could adsorb onto the surfaces of oppositely-charged AuNCs via electrostatic interactions to form “a drop” of fluorimetric reaction substrate. Furthermore, AChE was added into the above reaction substrate to catalyze the hydrolysis of ATC to produce thiocholine with positively charged and additional thiol (-SH) groups. The yielded thiocholine could then cap onto the BSA-AuNCs surfaces through electrostatic interactions, hydrogen bonds, and metal-thiol bonding. An

aggregation procedure of AuNCs would thus occur to cause a great decrease in the fluorescence intensities, which could depend on the catalysis activities of AChE. Alternatively, when OPs were applied into the reaction system, they could inhibit the catalysis activities of AChE aforementioned. As a result, thiocholine released from the AChE-catalyzed hydrolysis of ATC could decrease, so that the aggregation and fluorescence decreases of

BSA-AuNCs might be curbed to some degree. Therefore, the so proposed fluorimetric system, by way of “lab-on-a-drop” with biocompatible fluorescent nanoprobess of AuNCs, should be tailored for the evaluation of the AChE activities under physiologically simulated environment towards the analysis of OPs with high sensitivity and selectivity, as demonstrated afterwards.

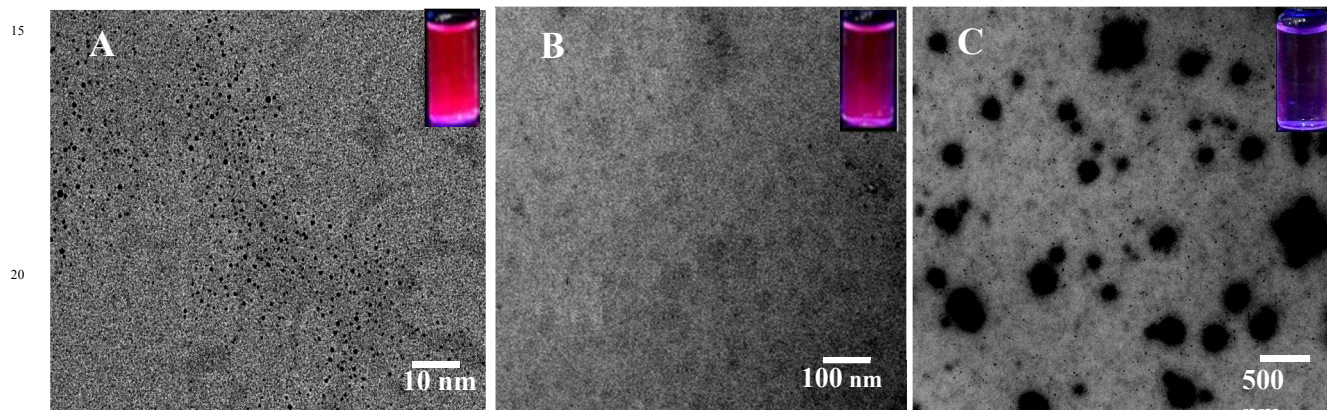


Fig. 1 TEM images of (A) AuNCs alone, and in the presence of (B) ATC, and (C) ATC with AChE.

3.2. Characterization of the AuNCs-based fluorimetric measurement procedure

In order to clarify the “lab-on-a-drop”-based fluorimetric procedure above, the characterization of morphology features of AuNCs was conducted by transmission electron microscopy (TEM) before and after the addition of ATC, followed by the AChE-catalyzed hydrolysis to release thiocholine (Fig. 1). It can be seen that the average size of AuNCs is about 0.8 nm (Fig. 1A). The addition of ATC to AuNCs might have little effect on the size of AuNCs (Fig. 1B), of which the AuNCs-ATC would serve as “a drop” of fluorimetric reaction substrate. Furthermore,

one can note that the introduction of AChE could induce the large aggregation of AuNCs (Fig. 1C). Accordingly, the TEM images supported the description and interpretations of AuNCs in the detection mechanism and procedure above. Moreover, the procedures were also monitored by fluorimetric measurements, where the fluorescence changes of reactants added by step-by-step way were recorded including fluorescence spectra, intensities and photographs (Fig. 2). As shown in Fig. 2A, the AuNCs displayed strong fluorescence at ~ 634 nm, corresponding to the fluorescence intensity in Fig. 2B (a) and the photographs (Insert). It was observed that when ATC was mixed with AuNCs, the fluorescence intensity could slightly

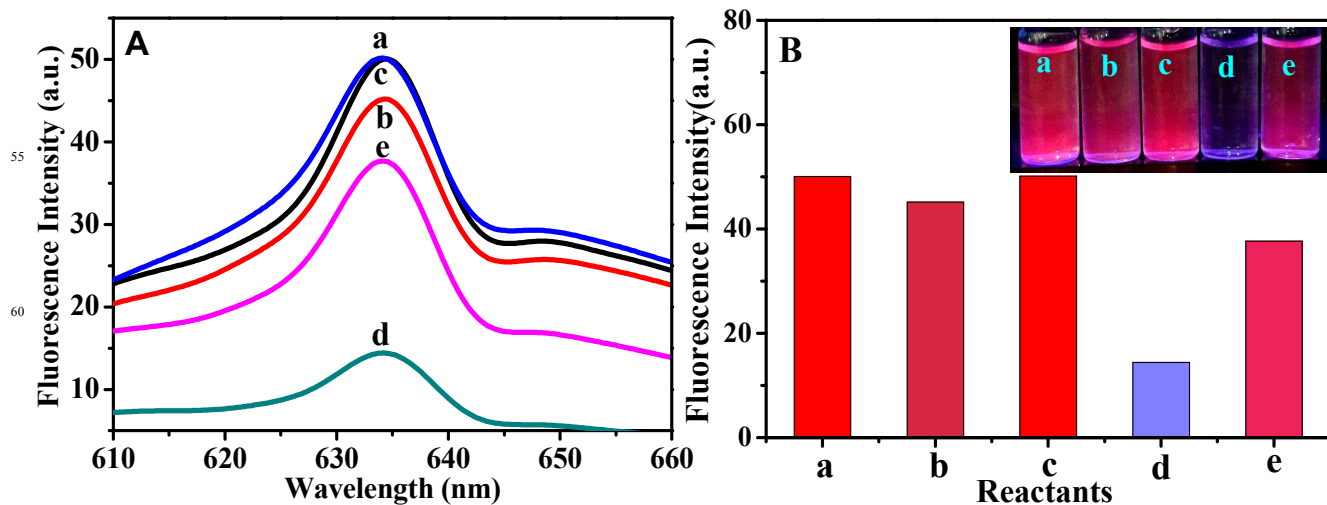


Fig. 2 (A) Fluorescence spectra and (B) corresponding fluorescence intensities of the reactants of (a) 1.25 mM AuNCs alone, and in the presence of (b) 50 μ M ATC, (c) 0.05 U / mL AChE, (d) 50 μ M ATC with 0.05 U / mL AChE, and (e) 50 μ M ATC with 0.05 U / mL AChE and 0.004 μ M DDVP, of which the reactants were added to AuNCs in step-by-step way (Inset: photographs under UV light).

decrease due to electrostatic interactions aforementioned (Fig. 2 A (b) and B (b)). Furthermore, the introduction of AChE could start the AChE-catalyzed hydrolysis of ATC to produce thiocholine. A greatly quenched fluorescence was observed, as clearly manifested in Fig. 2A (d) and B (d). But AChE showed no significant influence on the fluorescence of AuNCs (Fig. 2A (c) and B (c)). It demonstrates that the above fluorescence changes could result from AChE-catalyzed hydrolysis of ATC. However, when AChE was pre-exposed to a certain amount of DDVP, the decrease of the fluorescence of AuNCs was largely suppressed to some degree (Fig. 2A (e) and B (e)), due to the phosphorylation-induced inhibition of AChE catalysis activity. Of note, all fluorescence changes are in well consistent with photographs recorded under UV light (Fig. 2B (Inset)). Consequently, the “lab-on-a-drop”-based fluorimetric analysis

procedure could be established for the evaluation of AChE catalysis activity as well as the detection of OPs using biocompatible AuNCs as fluorescent nanoprobes.

3.3. Optimization of the reaction conditions of fluorimetric assays

The key detection conditions for the developed fluorimetric assays were optimized, including the amount of AuNCs, ATC concentrations, reaction time, and pH values (Fig. 3). Herein, the quenching efficiencies of AuNCs by thiocholine released from the AChE-catalyzed ATC hydrolysis were calculated according to the equation for quenching efficiencies defined with the details shown in the Experimental.

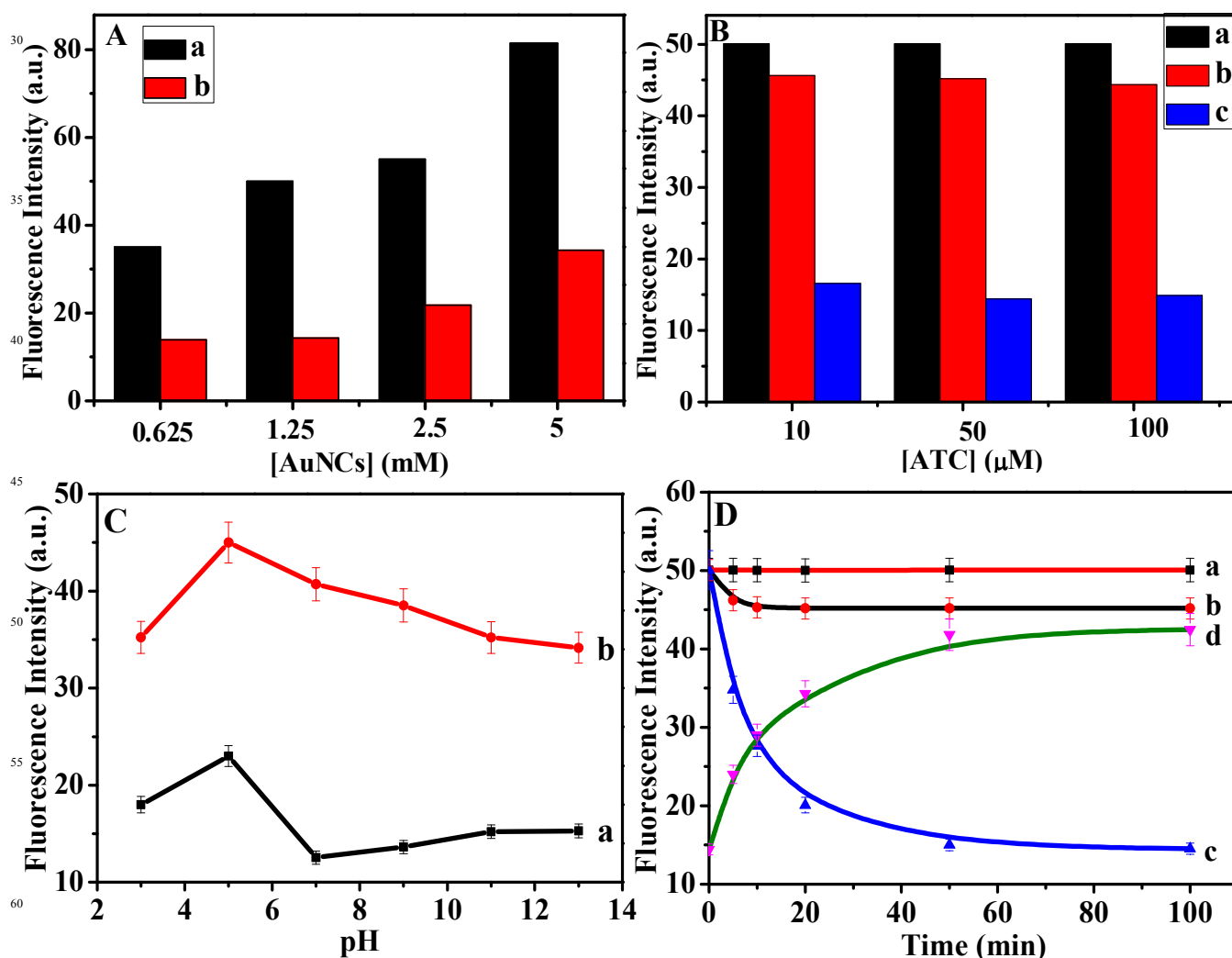


Fig. 3 (A) AuNCs concentration-dependent fluorescence intensities for (a) AuNCs alone of different concentrations, and (b) in the presence of 50 μM ATC and 0.05 U / mL AChE; (B) ATC concentration-dependent fluorescence intensities for (a) 1.25 mM AuNCs alone, and in the presence of (b) ATC of different concentrations, and (c) ATC of different concentrations with 0.05 U / mL AChE; (C) The pH-dependent fluorescence intensities for 1.25 mM AuNCs in the presence of (a) 50 μM ATC with 0.05 U / mL AChE, and (b) 50 μM ATC, 0.05 U / mL AChE, and 0.004 μM DDVP, of which the samples were incubated for 1h at different pH values; (D) Reaction time-dependent fluorescence intensities for (a) AuNCs alone, and in the presence of (b) 50 μM ATC, (c) 50 μM ATC and 0.05 U / mL AChE, and (d) 0.004 μM DDVP and AChE (0.05 U / mL), of which the reaction solution was taken out at the defined time intervals to be mixed with 50 μM ATC for fluorescence monitoring.

3.3.1 AuNCs amount for catalysis reactions

Since the sensitivity of the detection method is reflected by the variation of fluorescence intensity, the amount of AuNCs is an important factor. **Fig. 3A** shows the dependence of fluorescence intensities on the amounts of AuNCs with different concentrations which were calculated from the HAuCl_4 concentrations. With the increasing of AuNCs, the fluorescence increased gradually (**Fig. 3A (a)**). However, When ATC and AChE were applied in order, their fluorescence intensities could decrease with different quenching efficiencies (**Fig. 3A (b)**). Obviously, the highest quenching efficiency was obtained at the concentration of AuNCs of 1.25 mM, which is selected thereafter.

3.3.2 ATC concentration for catalysis reactions

Fig. 3B shows the effects of ATC concentrations on fluorescence intensities of AuNCs before (**Fig. 3B (b)**) and after (**Fig. 3B (c)**) the addition of AChE, where the original AuNCs was used as the control (**Fig. 3B (a)**). One can note that the highest quenching efficiency for the AChE-catalysis reaction solution could be achieved at 50 μM ATC, serving as the optimum one to be chosen. Higher ATC concentration (i.e., 100 μM) could show no significant change in fluorescence intensity. Yet, too high ATC concentration might have the risk of large accumulation of positively-charged ATC, resulting in the aggregation of AuNCs nanoprobe prior to the AChE catalysis reactions, as observed elsewhere for silver nanoparticles.³¹

3.3.3 The pH values of catalysis and phosphorylation reactions

The pH value is another important factor governing the fluorimetric detection system. **Fig. 3C** exhibits the pH-dependent fluorescence intensities of the reaction solutions of which the AChE catalysis and DDVP phosphorylation were conducted at different pH values. It was found that the highest fluorescence intensity might be obtained with a precipitation at $\sim \text{pH } 5.0$, presumably because of the charge neutrality of BSA-stabilized AuNCs (the isoelectric point of BSA at pH 4.7). But the suitable pH range for the AChE catalysis and DDVP phosphorylation

reactions are found from pH 7.0 to 9.0, as determined by the largest fluorescence quenching and inhibition efficiencies.

3.3.4 Reaction time of catalysis and phosphorylation reactions

Fig. 3D shows the plots of fluorescence intensities versus the reaction time for AChE catalysis and DDVP-induced phosphorylation reactions, with AuNCs and the fluorimetric reaction substrate of AuNCs and ATC as the controls. One can find that the two controls could show no significant changes in fluorescence intensities of AuNCs over time (**Fig. 3D (a)** and **(b)**). However, as time went by, the additions of AChE could make the fluorescence intensities decrease gradually to reach a plateau after 1 h (**Fig. 3D (c)**). Moreover, the reaction time for DDVP-inhibited AChE catalysis was also optimized as 1 h, during which the quenching of the fluorescence of AuNCs could be mainly suppressed by the DDVP phosphorylation of AChE (**Fig. 3D (d)**), showing the increasing fluorescent intensity.

3.4. Evaluation performances of the “lab-on-a-drop”-based fluorimetric assay system

Under the optimum experimental conditions, the capabilities of the fluorimetric assay system for the label-free evaluation of AChE catalysis activities were investigated. **Fig. 4A** displays the fluorescence spectra of the fluorimetric AuNCs-ATC reaction substrate and various usage of AChE. As shown in **Fig. 4A**, the fluorescence intensities of AuNCs could decrease gradually with increasing concentrations of AChE in catalysis activity units. The relationship between the AChE activity units and fluorescence quenching efficiencies, which were calculated according to the equation detailed in the Experimental, was described in **Fig. 4B**, corresponding to photographs under UV light (**Fig. 4B (Inset)**).

A linear range of AChE concentrations was obtained ranging from 5.0×10^{-6} to 5.0×10^{-2} U / mL ($R^2 = 0.9704$), with the detection limit down to 2.0×10^{-6} U / mL. Accordingly, with biocompatible fluorescent nanoprobe of AuNCs, the present fluorimetric method can allow for the evaluation of AChE catalysis activities under physiologically friendly environments so as to facilitate the catalysis inhibition-based detection of OPs

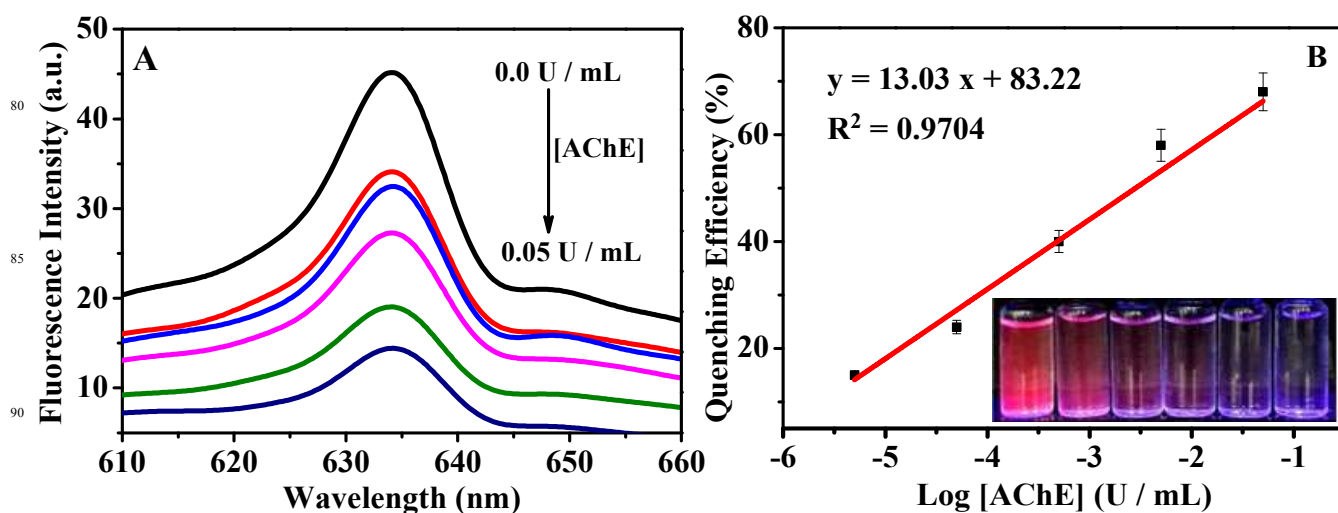


Fig. 4 (A) Fluorescence spectra of the fluorimetric reaction substrate (1.25 mM AuNCs and 50 μM ATC) in the presence of different AChE concentrations of 0.0, 0.000005, 0.00005, 0.0005, 0.005, and 0.05 U / mL; (B) Fluorescence quenching efficiencies versus the logarithmic activity units of AChE (Inset: photographs under UV light at 365 nm).

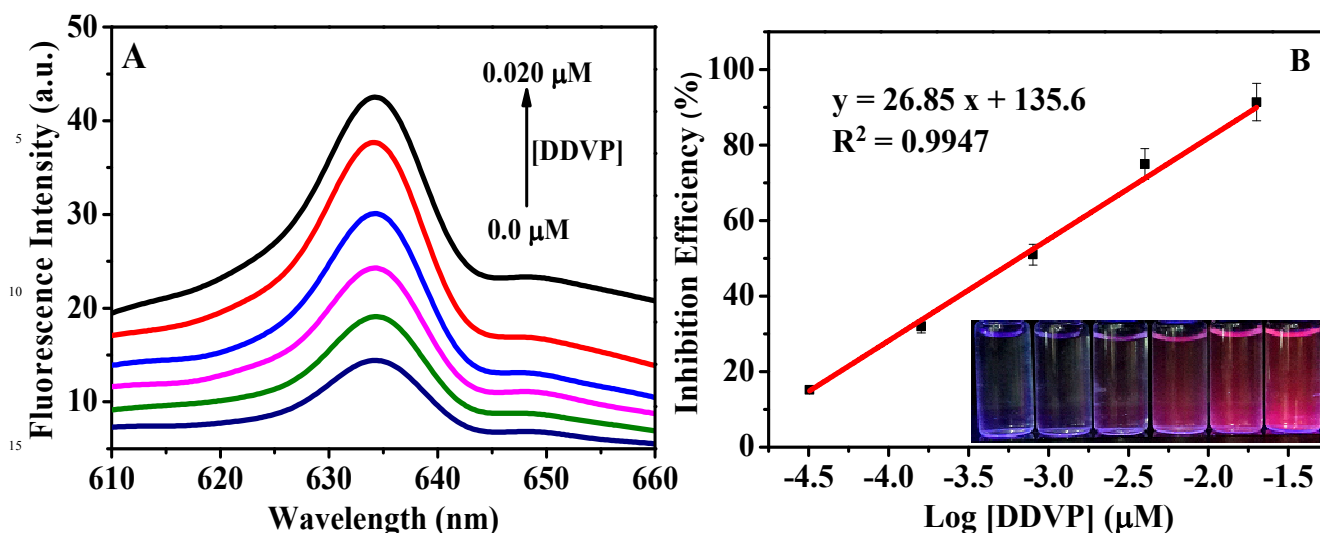


Fig. 5 (A) Fluorescence spectra of the catalysis reaction solution (1.25 mM AuNCs, 50 μM ATC, 0.050 U / mL AChE) mixed with DDVP of different concentrations of 0.0, 3.2×10^{-5} , 1.6×10^{-4} , 0.8×10^{-3} , 0.4×10^{-2} , and $2.0 \times 10^{-2} \mu\text{M}$; (B) The fluorescent inhibition efficiencies of DDVP versus the logarithmic concentrations of DDVP (Inset: photographs under UV light at 365nm)

with high sensitivity and selectivity, as demonstrated afterwards.

The quantitative detection abilities of the fluorimetric assay for DDVP as an OP model, were investigated on the basis of the phosphorylation-induced inhibitions of AChE catalysis activities (Fig. 5). As shown in Fig. 5A, the fluorescence intensities of AuNCs increased with increasing concentrations of DDVP, as also evidenced by the photographs under UV light (Fig. 5B (Insert)). The calibration curve was obtained with the DDVP concentrations linearly ranging from 3.2×10^{-5} to $2.0 \times 10^{-2} \mu\text{M}$ ($R^2 = 0.9947$), with the detection limit down to 13.67 pM (defined as the concentration of inhibitor required to achieve 5% inhibition),³² showing a considerably high detection sensitivity.

Moreover, the detection selectivity of the developed fluorimetric assay for DDVP was examined by using some potential interfering substance, including vitamin C (Vc), vitamin B₁ (V_{B1}), vitamin B₂ (V_{B2}), Fe³⁺, Na⁺, Mg²⁺, Zn²⁺, K⁺, Ca²⁺, PO₄³⁻, glucose (Glu), and fructose (Fru) (Fig. 6A). It is observed that comparing to DDVP, these common ions and organic compounds presented negligibly low inhibition efficiencies to the catalysis activity of AChE, indicating that they could show no interferences for the determination of DDVP under the optimized assay conditions. In addition, other kinds of OPs including the commonly used methidathion and paraoxon have also been tested,

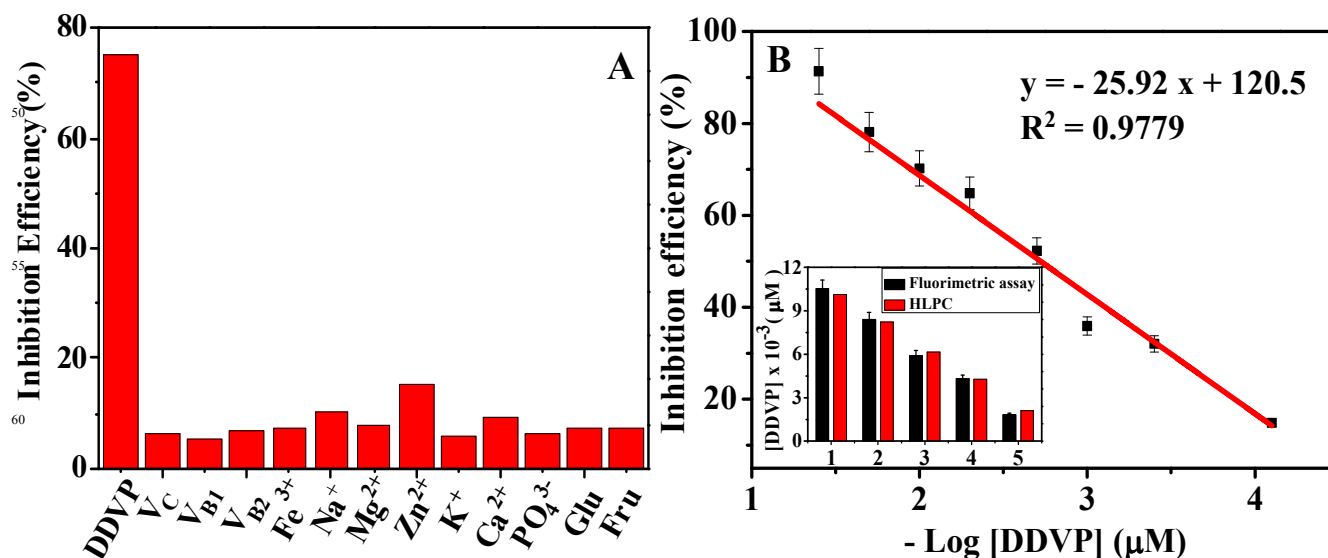


Fig. 6 (A) Comparison of fluorescent inhibition efficiencies among the potential interferents of 0.020 μM of vitamin C (Vc), vitamin B₁ (V_{B1}), Vitamin B₂ (V_{B2}), Fe³⁺, Na⁺, Mg²⁺, Zn²⁺, K⁺, Ca²⁺, PO₄³⁻, Glucose (Glu), and Fructose (Fru), comparing to 0.0040 μM DDVP, which were added into the fluorescence catalysis reaction solution (1.25 mM AuNCs, 50 μM ATC, and 0.05 U / mL AChE) to be measured under optimized conditions; (B) Calibration curve for the analysis of DDVP residues in vegetable samples of different concentrations (0.0, 8.0×10^{-5} , 4.1×10^{-4} , 0.12×10^{-2} , 0.23×10^{-2} , 0.51×10^{-2} , 1.2×10^{-2} , 2.2×10^{-2} , and $4.1 \times 10^{-2} \mu\text{M}$) by plotting the inhibition efficiencies versus the -logarithmic concentrations of DDVP, and the relation of analysis results between the HPLC and the fluorimetric assay for the detection of DDVP residues in vegetable samples (1 to 5) (Inset).

showing the inhibition efficiencies comparable to that of DDVP (data not shown). Accordingly, the developed AuNCs-based fluorimetric approach can determine total free OPs with high selectivity and anti-interference abilities.

3.5. Preliminary detection applications for DDVP residues in vegetable samples

To evaluate the feasibility of practical applications, the present fluorimetric assay was utilized for the detection of DDVP residues in samples of Chinese cabbage. Herein, the concentrations of DDVP residues in samples were first determined by using high-performance liquid chromatography (HPLC), and then diluted into different DDVP concentrations for the fluorimetric assays. The calibration curve for DDVP residues in samples was thus obtained, with the results shown in Fig. 6B. One can find that the -logarithmic concentrations of DDVP residues can linearly depend on the inhibition efficiencies (defined in the Experimental) in the range of 8.0×10^{-5} to 4.1×10^{-2} μM DDVP, with the detection limit down to ~ 36 pM. Of note, it is much lower than the maximum residue limits reported in the European Union pesticides database of 0.010 mg/kg (~ 64 pM) for DDVP (http://ec.europa.eu/sanco_pesticides). Moreover, a comparison of detection abilities between the classic HPLC and the developed fluorimetric assay was carried out for some DDVP residues-containing vegetable samples (Fig. 6B (Insert)), both showing a high relation in the analysis results. Therefore, the so developed “lab-on-a-drop”-based fluorimetric method can possess the potential of serving as a reliable and sensitive strategy for the detection of pesticide residues (i.e., DDVP) in real samples of vegetables.

4. Conclusions

In the present work, protein-stabilized AuNCs have been applied initially as biocompatible fluorescent nanoprobe for the label-free evaluation of the catalytic hydrolysis and phosphorylation of AChE under physiologically-simulated environments. “A drop” of fluorimetric reaction substrate consisting of AuNCs and ATC mixture was employed to facilitate the rapid “lab-on-a-drop” fluorimetric measurements (fluorescence quenching and inhibition efficiencies) to monitor the procedures of catalysis and phosphorylation-induced inhibition reactions of AChE, which were also characterized by high-resolution electronic microscopy imaging. Moreover, a simple, rapid yet highly sensitive and selective fluorimetric analysis method has thereby been successfully established for probing the exposures to total free OPs of pesticide residues in vegetables by using dimethyl-dichloro-vinyl phosphate (DDVP) as an example. Investigation results demonstrate that the developed AuNCs-based fluorimetric method can possess some outstanding advantages over the traditional detection methodologies in monitoring the AChE catalysis activities and the detection of free OPs. First, the use of biocompatible fluorescent nanoprobe of AuNC could allow for the evaluation of AChE catalysis activity under physiologically-simulated environments, thus avoiding the possible denaturation and toxic inactivity of AChE. Second, the combination of

efficient hydrolytic catalysis and specific phosphorylation inhibition of AChE activities with sensitive fluorimetric outputs could enable the detection of OPs with high selectivity and sensitivity (down to ~ 36 pM DDVP in vegetables); Third, simple and label-free analysis procedures (“a drop”) could facilitate the rapid detection of total free OPs. Therefore, such a “lab-on-a-drop”-based detection strategy may pave the way towards the wide applications for the evaluation of physiologic catalysis activities of various enzymes (i.e., cholinesterase) and especially for monitoring the direct phosphorylation biomarkers of free OPs towards rapid early warning and accurate diagnosis of the exposures to OPs in environment (i.e. pesticides), Warfield (i.e., nerve agents), and clinical laboratories.

Acknowledgments

This work is supported by the National Natural Science Foundations of China (No. 21375075, 21302109, and 21302110), the Taishan Scholar Foundation of Shandong Province, and the Natural Science Foundation of Shandong Province (ZR2013BQ017 and ZR2013BM007), P. R. China.

Notes and references

- ^a Shandong Province Key Laboratory of Life-Organic Analysis, School of Chemistry and Chemical Engineering, Qufu Normal University, Qufu City, Shandong Province 273165, P. R. China.
- ^b School of Mechanical and Materials Engineering, Washington State University, Pullman, WA 99164, USA.
- * Corresponding Author: E-mail addresses: huawangqfnu@126.com; Tel: +86 537 4456306; Fax: +86 537 4456306
1. H. Li, J. Guo, H. Ping, L. Liu, M. Zhang, F. Guan, C. Sun and Q. Zhang, *Talanta*, 2011, 87, 93-99.
2. F. Yang, J. R. Wild and A. J. Russell, *Biotechnol. Progr.*, 1995, 11, 471-474.
3. W. J. Donarski, D. P. Dumas, D. P. Heitmeyer, V. E. Lewis and F. M. Raushel, *Biochemistry*, 1989, 28, 4650-4655.
4. A. Fiddler, A. Hulst, D. Noort, R. De Ruiter, M. Van der Schans, H. Benschop and J. P. Langenberg, *Chem. Res. Toxicol.*, 2002, 15, 582-590.
5. L.-J. Qu, H. Zhang, J.-H. Zhu, G.-S. Yang and H. Y. Aboul-Enein, *Food Chem.*, 2010, 122, 327-332.
6. M. K. Chai and G. H. Tan, *Food Chem.*, 2009, 117, 561-567.
7. T. Pérez-Ruiz, C. Martínez-Lozano, V. Tomás and J. Martín, *Anal. Chim. Acta.*, 2005, 540, 383-391.
8. C. Padrón Sanz, R. Halko, Z. Sosa Ferrera and J. Santana Rodríguez, *Anal. Chim. Acta.*, 2004, 524, 265-270.
9. Y. Li, Z. Gan, Y. Li, Q. Liu, J. Bao, Z. Dai and M. Han, *Sci. China Chem.*, 2010, 53, 820-825.
10. Y. Zhang, H. Wang, J. Nie, Y. Zhang, G. Shen and R. Yu, *Biosens. Bioelectron.*, 2009, 25, 34-40.
11. H. Wang, J. Wang, C. Timchalk and Y. Lin, *Anal. Chem.*, 2008, 80, 8477-8484.
12. J. Gabaldon, A. Maquieira and R. Puchades, *Talanta*, 2007, 71, 1001-1010.
13. M. Wang, X. Gu, G. Zhang, D. Zhang and D. Zhu, *Langmuir*, 2009, 25, 2504-2507.
14. D. Liu, W. Chen, J. Wei, X. Li, Z. Wang and X. Jiang, *Anal. Chem.*, 2012, 84, 4185-4191.
15. Z. Chen, X. Ren and F. Tang, *Chin. Sci. Bull.*, 2013, 58, 2622-2627.
16. M. Wang, X. Gu, G. Zhang, D. Zhang and D. Zhu, *Anal. Chem.*, 2009, 81, 4444-4449.

17. S.-W. Zhang and T. M. Swager, *J. Am. Chem. Soc.*, 2003, 125, 3420-3421.
18. T. Yu, T.-Y. Ying, Y.-Y. Song, Y.-J. Li, F.-H. Wu, X.-Q. Dong and J.-S. Shen, *RSC Adv.*, 2014, 4, 8321.
- 5 19. R. Hardman, *Environ. Health Perspect.*, 2006, 165-172.
20. Z. Zheng, Y. Zhou, X. Li, S. Liu and Z. Tang, *Biosens. Bioelectron.*, 2011, 26, 3081-3085.
21. D. Du, W. Chen, W. Zhang, D. Liu, H. Li and Y. Lin, *Biosens. Bioelectron.*, 2010, 25, 1370-1375.
- 10 22. G. Zhang, Y. Li, J. Xu, C. Zhang, S. Shuang, C. Dong and M. M. Choi, *Sens. Actuators, B*, 2013, 183, 583-588.
23. J. Xie, Y. Zheng and J. Y. Ying, *Chem. Commun.*, 2010, 46, 961-963. 50
24. Y. Tao, Y. Lin, J. Ren and X. Qu, *Biosens. Bioelectron.*, 2013, 42, 41-46.
- 15 25. X. Xia, Y. Long and J. Wang, *Anal. Chim. Acta.*, 2013, 772, 81-86.
26. J. Xie, Y. Zheng and J. Y. Ying, *J. Am. Chem. Soc.*, 2009, 131, 888-889.
27. C. Guo and J. Irudayaraj, *Anal. Chem.*, 2011, 83, 2883-2889.
28. H. Liu, X. Zhang, X. Wu, L. Jiang, C. Burda and J.-J. Zhu, *Chem. Commun.*, 2011, 47, 4237-4239. 20
29. T. Pérez-Ruiz, C. Martínez-Lozano, V. Tomás and J. Martín, *Talanta*, 2001, 54, 989-995.
30. Z. Lin, F. Luo, T. Dong, L. Zheng, Y. Wang, Y. Chi and G. Chen, *Analyst*, 2012, 137, 2394-2399. 55
- 25 31. Z. Li, Y. Wang, Y. Ni and S. Kokot, *Sens. Actuators, B*, 2014, 193, 205-211.
32. J. Abad, F. Pariente, L. Hernandez, H. Abruna and E. Lorenzo, *Anal. Chem.*, 1998, 70, 2848-2855.

30

35

40

45